Journal of Solid State Chemistry 211 (2014) 90–94

Contents lists available at ScienceDirect

Journal of Solid State Chemistry

journal homepage: www.elsevier.com/locate/jssc

A novel 3D structure composed of strings of hierarchical TiO_2 spheres formed on TiO_2 nanobelts with high photocatalytic properties

Yongjian Jiang [a], Meicheng Li [a,b,*], Dandan Song [a], Xiaodan Li [a], Yue Yu [a]

[a] State Key Laboratory of Alternate Electrical Power System with Renewable Energy Sources, School of Renewable Energy, North China Electric Power University, Beijing 102206, China
[b] Suzhou Institute, North China Electric Power University, Suzhou 215123, China

ARTICLE INFO

Article history:
Received 4 October 2013
Received in revised form
20 November 2013
Accepted 1 December 2013
Available online 14 December 2013

Keywords:
Titanium dioxide
Strings of hierarchical spheres
TiO_2 nanosheets
Photocatalytic

ABSTRACT

A novel hierarchical titanium dioxide (TiO_2) composite nanostructure with strings of anatase TiO_2 hierarchical micro-spheres and rutile nanobelts framework (TiO_2 HSN) is successfully synthesized via a one-step hydrothermal method. Particularly, the strings of hierarchical spheres are assembled by very thin TiO_2 nanosheets, which are composed of highly crystallized anatase nanocrystals. Meanwhile, the HSN has a large surface area of 191 m^2/g, which is about 3 times larger than Degussa P25. More importantly, the photocatalytic activity of HSN and P25 were evaluated by the photocatalytic oxidation decomposition of methyl orange (MO) under UV light illumination, and the TiO_2 HSN shows enhanced photocatalytic activity compared with Degussa P25, as result of its continuous hierarchical structures, special conductive channel and large specific surface area. With these features, the hierarchical TiO_2 may have more potential applications in the fields of dye-sensitized solar cells and lithium ion batteries.

1. Introduction

Titanium dioxide (TiO_2) is a versatile material and has been investigated considerably due to its various applications including photocatalysis [1], solar cells [2], sensors [3], and electron field emitter [4]. In the photocatalytic field, it is well-known that the crystalline anatase polymorph displays a higher photoactivity than rutile or brookite [5]. In recent years, more and more researchers have focused their attention on the controllable fabrication of anatase TiO_2. Up to now, kinds of TiO_2 morphologies have been synthesized, such as nanoparticles, nanorods, nanowires, nanosheets, nanoflowers, nanospheres [6–11], and so on. Among these TiO_2 morphologies, one-dimensional (1D) nanostructure can provide direct conductive paths and reduce the electron recombination; Two-dimensional (2D) nanosheets or nanowalls of TiO_2 with a high surface area are suggested to be used as ideal objects for the nanodevices in photoelectronic or photocatalytic fields; Three-dimensional (3D) nanostructures (e.g. TiO_2 nanosheet spheres or TiO_2 nanorod spheres) have good light absorption capability by permitting more lights reflection and multiple-scattering inside their structures, they also have the enhanced charge transfer facilitated by 1D or 2D nanostructure thus retarding the recombination of photogenerated electrons and holes [12–14]. Considering the above advantages of 1D, 2D, and 3D nanostructures, the synthesis of the combining nanostructures (1D, 2D, and 3D) which will have a better comprehensive performance, is very interesting.

Pre-sensitized TiO_2 nanobelts were prepared with the method provided in Ref. [15]. Compared to Degussa P25, because of its smaller specific surface area, the 1D TiO_2 nanobelts present a little better photocatalytic activity. Therefore, it is necessary to build a new kind of nanostructure to solve this problem. In this work, the strings of combinated nanostructures composed of 3D anatase hierarchical spheres on the axis of 1D nanobelt (TiO_2 HSN) have been synthesized for the first time. In the growth process, the 1D nanobelt acts as the growing framework, and it is decorated by strings of TiO_2 microspheres successfully. Furthermore, the assembled material has relatively large specific surface areas of 191 m^2/g, even comparable to the ordered mesoporous TiO_2 obtained from soft-templating route. Interestingly, as the novel nanostructure is able to combine the advantages of 1D, 2D and 3D structures, it is worthy to note that the synthesized TiO_2 HSN exhibits higher photocatalytic activity than Degussa P25.

2. Experimental

The composite nanostructures were synthesized from hydrolysis of tetrabutyl titanate (TBOT) on nanobelt, with CH_3COOH as the hydrothermal solvents. The nanobelts which served as substrates guide the growth of secondary TiO_2 nanostructures. The SEM of the nanobelt (several micrometers long and tens of nanometers wide) is shown in Fig. S2(a) (EIS). In a typical process, the nanobelt was

* Corresponding author. Tel./fax: +86 10 61772951.
E-mail addresses: mcli@ncepu.edu.cn, lmc50@cam.ac.uk (M. Li).

0022-4596/$ - see front matter © 2013 Elsevier Inc. All rights reserved.
http://dx.doi.org/10.1016/j.jssc.2013.12.002

put into an autoclave containing the mixed solutions of TBOT–$AgNO_3$–CH_3COOH with 0.5 ml TBOT, 0.1 g $AgNO_3$ and 40 ml CH_3COOH. The mixed solution was stirred for 30 min to generate a homogeneous solution, and then transferred to a high pressure reactor. Hydrothermal synthesis was conducted at 150 °C for 6 h. After the hydrothermal treatment, the synthesized product was washed with de-ionized water and calcined at 450 °C for 30 min.

Photocatalytic activity experiments of the HSN were conducted by degradation of methyl orange (MO) at room temperature. A 20 W UV lamp was used as the irradiation source. In photocatalytic testing, 100 mg/l of the obtained TiO_2 HSN powder was dispersed in 20 mg/l MO dye solution. For comparison, the experiment was done on Degussa P25 in the same way. Before the irradiation, the reaction systems were put by continuous stirring for 2 h to reach the adsorption balance, and these two solutions were used to measure the adsorption ability of HSN and Degussa P25. Then this two mixed solutions were exposed to UV light irradiation, and each sample's supernatant liquid was extracted every 30 min for further MO content testing. As a better contrast, photocatalytic experiments on Degussa P25, TiO_2 HSN and TiO_2 nanobelt were conducted after 120 min degradation reaction. The concentration of MO was measured with a UV–vis spectrophotometer and the absorbance at 465 nm was monitored.

3. Results and discussion

The strings of TiO_2 hierarchical spheres on TiO_2 nanobelt (HSN) were fabricated through a hydrothermal process as outlined in the experimental section. Fig. 1 shows the corresponding SEM and TEM images of as-prepared product. Fig. 1a and b are typically low and high magnification SEM images of the as-prepared product. As shown in Fig. 1a, the TiO_2 micro-spheres are neatly arranged on the nanobelts, forming a sphere-ribbon structure with an average diameter of 500 nm/μm, and the nanobelts act as growing frameworks, surrounded by a large number of microspheres, as shown in Fig. 1c. To better analyze the crystallographic structures, the obtained TiO_2 HSN and the TiO_2 nanobelt frameworks were both investigated by X-ray diffraction. As indicated by the XRD patterns (Fig. 2a), for the sample of TiO_2 nanobelt frameworks (the above line), we can find three diffraction peaks, and they are able to be ascribed to 110, 103, and 220 faces of the tetragonal rutile TiO_2 (JCPDS No. 21-1272), which are the results of partly crystallized TiO_2 product. In addition, from the XRD patterns (the line below) of the as-prepared samples obtained after hydrothermal and calcination reactions, obvious humps of (1 0 1) face at 2θ of 25.37 and (2 0 0) face at 2θ of 48.12 can be detected. Compared with the XRD pattern of TiO_2 nanobelt frameworks, the XRD pattern of HSN demonstrates the existence of anatase TiO_2. As we know, the TiO_2 nanobelt frameworks have not changed after experimental process [15]. Therefore, it can be suggested that the formed TiO_2 in the reaction systems is anatase TiO_2.

Meanwhile, as shown in Fig. 1b, the micro-spheres composed of TiO_2 nanosheet blocks, and all of the nanosheets are tetragonal in shape with a thickness of 10 nm and the side length of roughly 200 nm. TEM image (Fig. 1d) also reveals that the inter-meshed nanopetals of 3D hierarchical spherical TiO_2, and these nanopetals consist of interconnected nanosheets. The inserted selected area electron diffraction (SAED) pattern (inset Fig. 2b) further confirms its polycrystalline nature of the spherical anatase TiO_2 nanostructures. Particularly, in the corresponding high-resolution TEM (HRTEM) image (Fig. 2b), (1 0 1) and (0 0 1) crystalline planes with the interplanar spacings of 0.35 nm and 0.236 nm which are well consistent with the previous XRD results, can be clearly observed.

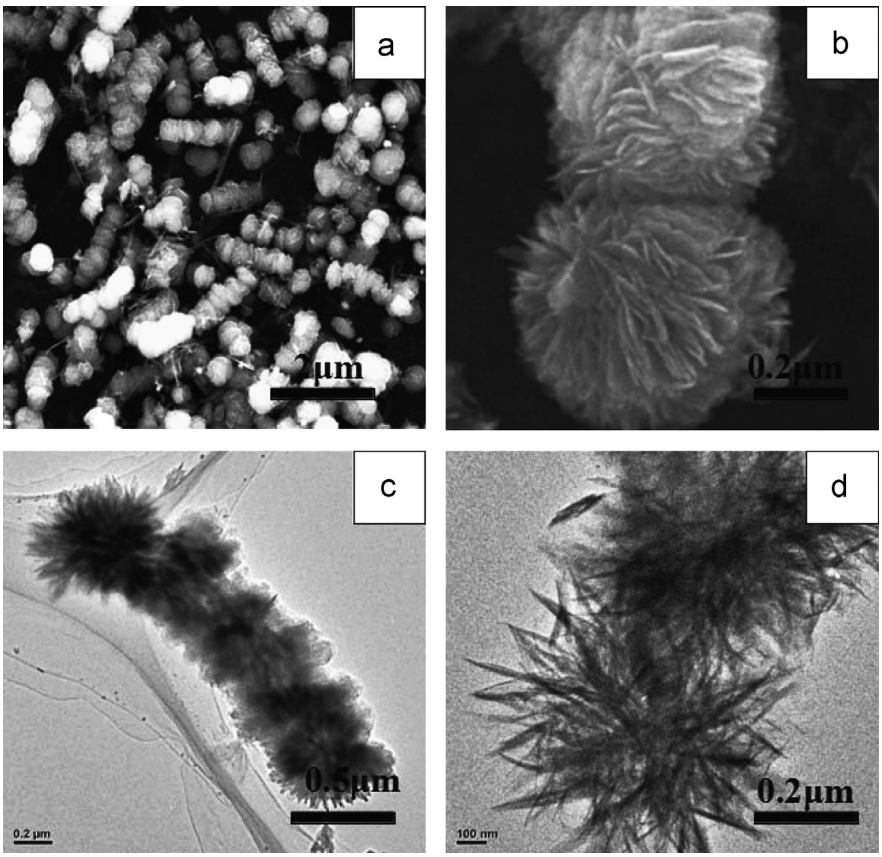

Fig. 1. (a) and (b) SEM images and (c) and (d) TEM images of the HSN synthesized at 150 °C for 6 h.

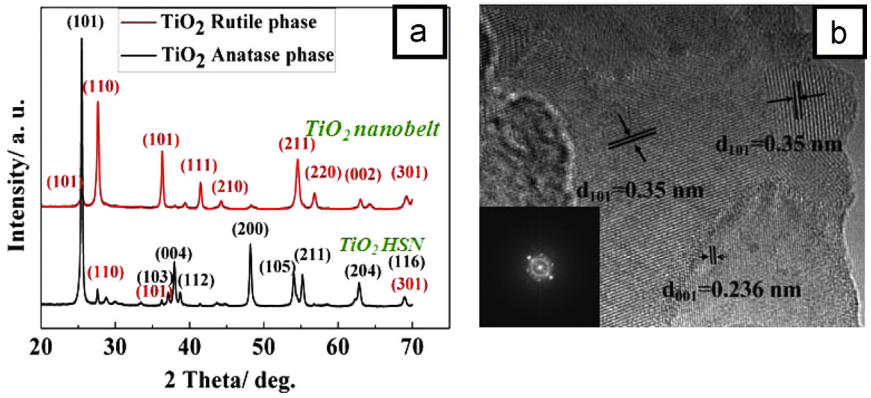

Fig. 2. (a) XRD patterns of the prepared TiO_2 HSN and the TiO_2 nanobelt framwork. The red labels correspond to rutile phase, and the black labels correspond to anatase phase; HRTEM (Fig. 1 (b) and the electron diffraction pattern (inset Fig. 1 (b) images of the calcined HSN obtained from 6 h hydrothermall reaction. (For interpretation of the references to color in this figure legend, the reader is referred to the web version of this article.)

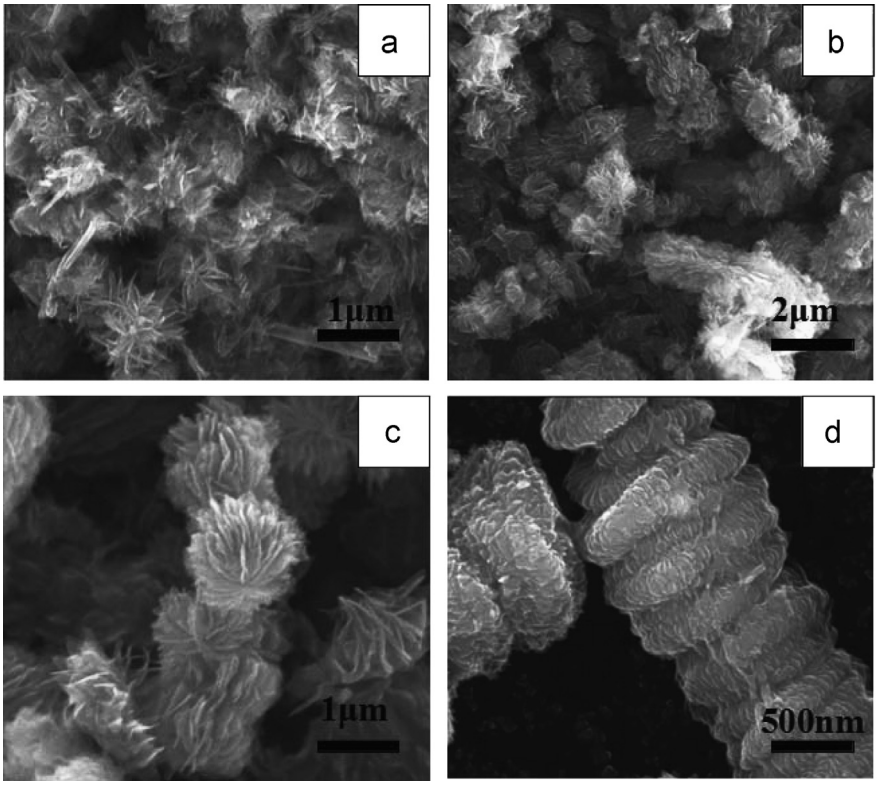

Fig. 3. SEM images of the products synthesized at 150 °C for (a) 2 h; (b) 4 h; (c) 6 h; (d) 8 h.

To study the morphological evolution of TiO_2 HSN nanostructures, time-dependent experiments (the reaction times were 2 h, 4 h, 6 h and 8 h) were done. The products prepared at different growth stages were examined by SEM. As shown in Fig. 3a, only nanosheets were obtained at the early stage (2 h). When the reaction time was prolonged to 4 h, TiO_2 nanosheet strings structures began to appear on TiO_2 nanobelts (Fig. 3b). When the reaction time was further up to 6 h, relatively hierarchical microspheres growing uniformly on the TiO_2 nanobelts (HSN) were obtained, which composed of the nanosheet units (Fig. 3c). As the reaction proceeded, TiO_2 hierarchical microspheres gradually tended to crowd together, as shown in Fig. 3d. Finally, well-defined TiO_2 HSN nanostructures were formed after the reaction time of 6 h. Additionally, the composition and contents of the obtained samples were investigated by EDS measurement. The EDS results reveal that the only elementary components are Ti and O, as shown in Fig. S1 (ESI†).

Apart from reaction time, the role of the coexistence of TiO_2 nanobelts, $AgNO_3$, TBOT and CH_3COOH was found to be critical in the morphology control. In the control experiments, when no TiO_2 nanobelts were added, neither TiO_2 3D hierarchical spheres nor 2D nanosheets were observed, but only nanosized particles were obtained by the hydrolysis of TBOT (Fig. 4a). It is widely recognized that the epitaxial and anisotropic nucleation and growth can be induced by the atom arrangement at the nucleation site on substrate and precursor [16,17]. Notably, the TiO_2 nanobelt has a tetragonal rutile structure, and such small lattice mismatch promoted the epitaxial nucleation and growth compactly on rutile TiO_2 Nanobelt. So we can say that the TiO_2 nanobelts serve as an important growth framework, and the nanobelts play a significant role in promoting the nucleation, growth

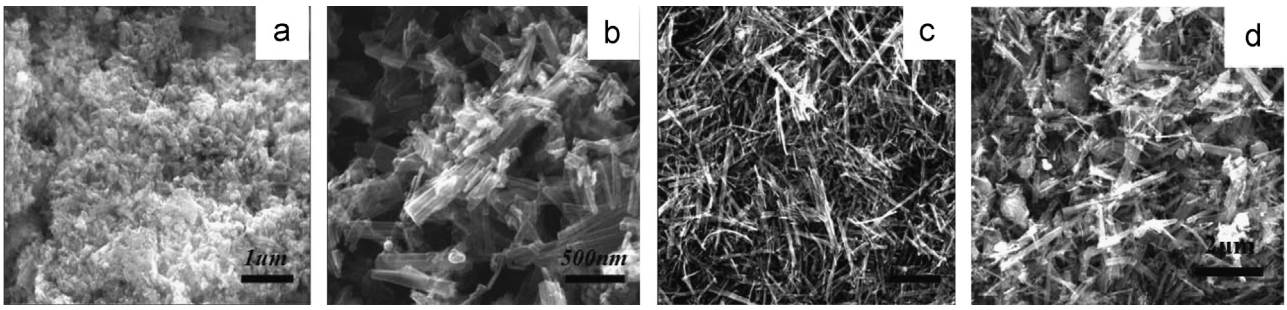

Fig. 4. SEM images of the product prepared from hydrothermal process at 150 °C for 6 h: (a) without the use of TiO_2 nanobelt; (b) without the use of $AgNO_3$; (c) without the use of TBOT; (d) deionized water act as the reaction solvent instead of glacial acetic acid.

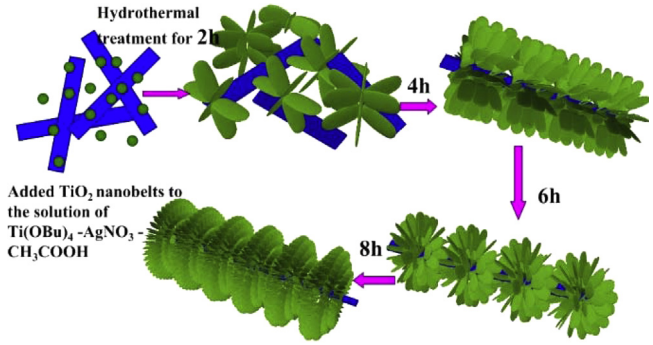

Fig. 5. Schematic illustration of the TiO_2 hierarchical architectures formation procedure.

and aggregation of TiO_2 nanosheets. When no $AgNO_3$ was added, only glacial acetic acid and TBOT existed as reactants, and not 3D hierarchical sphere or nanosheets but one-dimensional (1D) thicker nanorod can be found (Fig. 4b). It indicates that further dissolution–renucleation and growth process for the microspheres do not happen because of the absence of $AgNO_3$. Moreover, the addition of cations greatly increased the ionic strength of the reaction solution, which favored the formation of small crystals of TiO_2 through electrostatic screening [18]. Thus, in this work, the addition of Ag^+ ions led to the creation of hierarchical micro-spheres TiO_2 architectures instead of 1D thicker nanorods. When no TBOT was added, in fact, with little changed on the nanobelts (Fig. 4c), it can be confirmed that the 3D hierarchical spheres of the HSN all come from the hydrolysis product of TBOT. When the reaction solvent of acetic acid was replaced by deionized water, the product was some TiO_2 particle and nanobelt, and no nanosheet or micro-sphere appeared. We propose that the acetic acid significantly reduced the hydrolysis rate of TBOT, and acetic acid have played an important role in controlling morphology of TiO_2 nanostructures [10].

On the basis of the above experimental facts, we propose the following mechanism which is illustrated in Fig. 5. The formation process based on the experiment results can be divided into four steps: (1) formation and growth of small nanosheets on nanobelts; (2) nanosheets grow thicker and larger and begin to form sphere-like structures; (3) micro-spheres grow neatly on the frameworks of nanobelts; (4) TiO_2 hierarchical nanostructures gradually tend to crowd together and get squashed.

Considering the special hierarchical and continuous TiO_2 nanostructures, the physical properties of the S_{BET} was measured for further photocatalytic activity research. Compared with Degussa P25, the HSN shows a higher S_{BET} of 191 m^2/g, while the S_{BET} of P25 and TiO_2 nanobelt are only 59 m^2/g and 21 m^2/g, respectively. Based on its large specific surface area and special structure, photocatalytic activity test was done and the same experiment was also done on Degussa P25 for comparison by UV-light degradation of MO. Before the irradiation, the reaction system was continuously stirred for 2 h to reach the adsorption balance [19], and these two solutions were used to measure the adsorption data of HSN and Degussa P25. As shown in Fig. 6a, HSN shows a adsorption proportion as high as 44%, about 2 times higher than that of P25 (24%), which attributed to its larger specific surface area.

After that, upon irradiation, this novel TiO_2 product also shows a distinctly more rapid degradation rate than that of P25. It can be seen from Fig. 6b, with HSN, a 65 percent degradation of MO is achieved after 3 h irradiation, which is 30% higher than the degradation of Degussa P25. To further verify the necessity of synthesis of the novel TiO_2 nanostructure, the catalytic properties of TiO_2 nanobelt framework have also been researched. As shown in Fig. S2(b) (ESI†), the HSN presents the best photocatalytic performance, and TiO_2 nanobelt presents just a little better photocatalysis than P25. Even more interesting, the adsorption spectra of MO present a red shift phenomenon due to the existence of the novel TiO_2 HSN. The reasons for this phenomenon may be explained as that the new structure (HSN) altered the organic groups in MO, and the roles HSN played in the change of MO adsorption spectra are still under investigation.

Based on the above results, the HSN presents enhanced photocatalytic activity, which should be related to its interesting strings structure. The novel TiO_2 nanostructure composed of three kind of dimensional structures (TiO_2 1D, 2D and 3D nanostructure) simultaneously: 1D nanobelts act as a special conductive channel to connect the 3D hierarchical structures; 2D nanosheets propose large specific surface area so as to increase the adsorption of organic molecules; 3D micro-spheres provide more active sites and increase the capture of light. With the above advantages combined, it is clearly shown that the nanostructure of hierarchical anatase TiO_2 spheres on rutile nanobelts (HSN) with loose structures is an excellent photocatalyst material.

4. Conclusions

In summary, a simple one-step approach of strings of TiO_2 nanostructures composed of micro-spheres orderly growth on the TiO_2 nanobelts has been presented. With very large S_{BET} and the hierarchical structure, the novel TiO_2 material exhibits better photocatalytic performance for the degradation of methyl orange compared with Degussa P25. On the one hand, more reaction sites are created in TiO_2 HSN which can be indicated by its larger surface area, and the 1D nanobelts act as the channels of electrons. On the other hand, HSN has a better crystallization degree of anatase phase. Combining these advantages, this kind of novel superstructure is also expected to have potential applications in catalyst support, solar cells and gas sensing.

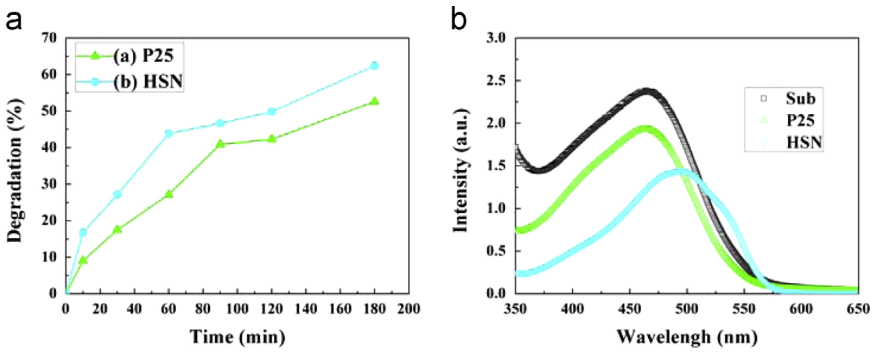

Fig. 6. (a) UV–vis adsorption spectra of the P25 and TiO_2 HSN after stirring in the dark in MO solution for 120 min at room temperature; (b) the curves between degradation ratio and degradation time. (a) Degussa P25; (b) TiO_2 HSN.

Acknowledgments

This work was supported by the National Natural Science Foundation of China (Grant nos. 91333122, 51372082, 51172069), and Ph.D. Programs Foundation of Ministry of Education of China (20130036110012, 20110036110006), and the Fundamental Research Funds for the Central Universities (Key project 11ZG02). We also would like to thank Prof. Hong Liu of Shandong University for his help about the preparation of TiO_2 nanobelts.

Appendix A. Supporting information

Supplementary data associated with this article can be found in the online version at http://dx.doi.org/10.1016/j.jssc.2013.12.002.

References

[1] A. Fujishima, K. Honda, Nature 238 (1972) 37.
[2] B. O'Regan, M. Gratzel, Nature 353 (1991) 737.
[3] X.J. Lü, F.Q Huang, X.L. Mou, Y.M. Wang, F.F. Xu, Adv. Mater. 22 (2010) 3719–3722.
[4] M.A. Shannon, P.W. Bohn, M. Elimelech, J.G. Georgiadis, B.J. Marinas, A. M. Mayes, Nature 452 (2008) 301.
[5] Z.K. Zheng, B.B. Huang, J.B. Lu, X.Y. Qin, X.Y. Zhang, Y. Dai, Chem. Eur. J. 17 (2011) 15032–15038.
[6] Y.Z. Dong, K. Pan, G.H. Tian, W. Zhou, Q.J. Pan, T.F. Xie, D.J. Wang, H.G. Fu, Dalton Trans. 40 (2011) 3808–3814.
[7] H.W. Bai, Z.Y. Liu, L. Liu, D.S. Darren, Chem. Eur. J. 19 (2013) 3061–3070.
[8] R. Raed, W. Atul, C. Dongkyu, F. Aziz, O.C. Samy, P. Umesh, P. Vivek, RSC Adv. 2 (2012) 7048–7052.
[9] J.G. Yu, J.J. Fan, L. Kangle, Nanoscale 2 (2010) 2144–2149.
[10] M.C. Li, Y.J. Jiang, R.Q. Ding, D.D. Song, H. Yu, Z. Chen, J. Electron. Mater. 42 (2013) 6.
[11] X.J Lü, S.J. Ding, Y. Xie, F.Q. Huang, Eur. J. Inorg. Chem. (2011) 2879–2883.
[12] A. Guo, W.T. Sun, Y.L. Zhang, L.M. Peng, Chem. Commun. 47 (2011) 6608–6610.
[13] J.J. Yuan, H.D. Li, Q.L. Wang, Q. Yu, X.K. Zhang, H.J. Yu, Y.M. Xie, Mater. Lett. 81 (2012) 123–126.
[14] Y.J. Jiang, M.C. Li, R.Q. Ding, D.D. Song, T. Mwenya, Z. Chen, Mater. Lett. 06 (2013) 009.
[15] Y.M. Wang, G.J. Du, H. Liu, D. Liu, S.B. Qin, N. Wang, C.G. Hu, X.T. Tao, J. Jiao, J.Y. Wang, Z.L. Wang, Adv. Funct. Mater. 18 (2008) 1131.
[16] X.F. Yang, C.J. Jin, C.L. Liang, D.H. Chen, M.M. Wu, J.C. Yu., Chem. Commun. 47 (2011) 1184.
[17] M. Shang, W.Z. Wang, W.Z. Yin, J Ren, S.M. Sun, L. Zhang, Chem. Eur. J. 16 (2010) 11412.
[18] M.D. Ye, H-Y. Liu, C.J. Lin, Z.Q. Lin, Small 9 (2013) 312–321.
[19] R.Y. Zhang, B. Tu, D.Y. Zhao, Chem. Eur. J. 16 (2010) 9977–9981.